Available online at www.sciencedirect.com
ScienceDirect
Journal of Magnetic Resonance 184 (2007) 322–329
JMR Journal of Magnetic Resonance
www.elsevier.com/locate/jmr

Communication

Improved resolution in ^{13}C solid-state spectra through spin-state-selection ☆

René Verel, Theofanis Manolikas, Ansgar B. Siemer, Beat H. Meier *

Physical Chemistry, ETH Zurich, Wolfgang-Pauli-Strasse 10, CH-8093 Zurich, Switzerland

Received 14 July 2006; revised 21 September 2006
Available online 7 November 2006

Abstract

The application of a spin-state-selective coherence transfer experiment (INADEQUATE-SSS) to solid-state NMR spectroscopy is described. Two-dimensional ^{13}C double-quantum/single-quantum spectra without J splittings in both dimensions lead to enhanced spectral resolution. The method is demonstrated to significantly improve the spectral resolution of the crowded C'–C^{α} region of two proteins.

Keywords: Solid-state NMR; Spin-state selection; High resolution

1. Introduction

Recent advances in heteronuclear decoupling pulse techniques [1–5] and attention to sample preparation [6,7] have improved the resolution of ^{13}C solid-state MAS NMR spectra in uniformly labelled peptides and proteins to the point that it now is limited by non-resolved or partially resolved homonuclear J couplings. A somewhat similar situation is encountered in ^{13}C detected liquid-state spectra [8].

Several methods have been developed to remove the J splitting from the spectra. For the indirect dimension of multi-dimensional spectra, homonuclear decoupling using a selective refocusing pulse has been shown to be a robust and easy to implement method [9,10]. Of even grater interest is the decoupling in the directly detected dimension where high spectral resolution comes without increased measurement time. Different approaches to this problem have been discussed in the literature. One approach uses selective homonuclear decoupling during acquisition and involves the switching between acquisition of a data point and application of rf close to the observation frequency [11–15]. This approach is technically challenging and the obtained signal-to-noise ratio is compromised because no samples can be taken during the pulse and the pulse ringdown period. The second approach, the one to be further developed in this paper, employs pulse techniques to prepare a spin state of the type $\hat{S}_{i,y}\hat{S}_j^{\beta}$ before the actual data acquisition [16–18]. Such states lead to an NMR spectrum where only one line of a spin doublet is visible, in our example, one line of the i-spin doublet produced by a J-coupling term between spins i and j. The application of spin-state selection schemes to MAS NMR of solids [19], specifically the IPAP scheme [20,21], has already been demonstrated [22,23].

Spin-state selective methods are most easily applied to spins that have only a single coupling partner with a sizeable J coupling. This is the case for the carbonyl resonances in peptides or proteins. Incidentally, an improved resolution in the crowded C'–C^{α} cross peak region is of great practical importance for the assignment process in peptides and proteins.

In this communication, a spin-state-selective version of the INADEQUATE experiment is described. The polarization transfer occurs via the J coupling. After a short theoretical description of the spin-state-selective conversion of double-quantum (DQ) to single-quantum (SQ) coherence,

☆ Presented, in part at the 47th ENC, Asilomar, CA, April 2006.

* Corresponding author. Fax: +41 44 632 1621.
E-mail address: beme@ethz.ch (B.H. Meier).

1090-7807/$ - see front matter
doi:10.1016/j.jmr.2006.09.024

the remainder of this paper will focus on the practical characterization and implementation of the experiment. The basic principles will be illustrated on the model compound glycine ethyl ester and the practical relevance will be discussed with data from two different protein samples: ubiquitin, a small globular protein consisting of 76 amino acid residues [24] and the fragment 218–289 of the HET-s prion protein [25].

2. Theory

In the following, a greatly simplified two-spin Hamiltonian is used to describe the principles of the spin-state-selection experiment. Assuming that MAS is fast enough to average out all spatially anisotropic interactions, we consider, in the following, only the isotropic part of the chemical shift and the isotropic part of the J coupling. Considering the small size of the ^{13}C–^{13}C J coupling, when compared to typical chemical-shift differences, we further invoke the weak-coupling approximation and use the model Hamiltonian $\mathscr{H} = \omega^{(1)}\hat{S}_{1,z} + \omega^{(2)}\hat{S}_{2,z} + 2\pi J\hat{S}_{1,z}\hat{S}_{2,z}$, where $\omega^{(i)}$ is the isotropic chemical shift of spin i.

With these simplifications the behavior of a C'–C^{α} spin pair can be analyzed in the framework of the product-operator formalism [26]. The experimental pulse scheme to be discussed is shown in Fig. 1. The experiment starts with an adiabatic cross-polarization step [27] from protons to ^{13}C leading to an initial carbon density operator $\sigma(0) \propto \hat{S}_{1,y} + \hat{S}_{2,y}$. The τ_1 period generates DQ coherence using the INADEQUATE scheme [28–30]. For perfect $\pi/2$ and π pulses (all with phase along x) and a delay $\tau_1/2$ adjusted to $1/4J$ we are left with pure DQ coherence at the end of the τ_1 period: $\sigma(\tau_1) \propto \hat{S}_1^+\hat{S}_2^+ - \hat{S}_1^-\hat{S}_2^-$. The DQ coherence evolves during t_1 and is reconverted to single-quantum coherence of the form $\hat{S}_1^-\hat{S}_2^{\beta}$. This can be achieved by the SSS sequence [(selective $\pi/2$) - $\tau_2/2$ - π - $\tau_2/2$ - (selective $\pi/2$)] first described by Sørensen and coworkers [18] with $\tau_2/2 = 1/4J$. The rotation operator which formally achieves this transformation (equal to an selective pulse on the $|\alpha\alpha\rangle$ to $|\beta\alpha\rangle$ transition) is a π rotation with $\hat{S}_1^{\alpha}\hat{S}_{2,y}$. Following the scheme described by Sørensen et al. [18] we rewrite this rotation operator as

$$\begin{aligned}
exp(i\pi\hat{S}_1^{\alpha}\hat{S}_{2,y}) &= \exp\left(\frac{i\pi}{2}(2\hat{S}_{1,z}\hat{S}_{2,y} + \hat{S}_{2,y})\right)\\
&= \exp\left(\frac{i\pi}{2}\hat{S}_{2,x}\right)\exp\left(\frac{i\pi}{2}2\hat{S}_{1,z}\hat{S}_{2,z}\right)\\
&\quad\times\exp\left(\frac{-i\pi}{2}\hat{S}_{2,x}\right)\exp\left(\frac{i\pi}{2}\hat{S}_{2,y}\right)\\
&= \exp\left(\frac{i\pi}{2}\hat{S}_{2,x}\right)\exp\left(\frac{i\pi}{2}2\hat{S}_{1,z}\hat{S}_{2,z}\right)\\
&\quad\times\exp(i\pi(\hat{S}_{1,x} + \hat{S}_{2,x}))\exp(i\pi\hat{S}_{1,x})\\
&\quad\times\exp\left(\frac{i\pi}{2}\hat{S}_{2,y}\right)\exp\left(\frac{-i\pi}{2}\hat{S}_{2,z}\right)\\
&= \exp\left(\frac{i\pi}{2}\hat{S}_{2,x}\right)\exp(i\hat{\mathscr{H}}/4J)\\
&\quad\times\exp(i\pi(\hat{S}_{1,x} + \hat{S}_{2,x}))\exp(i\hat{\mathscr{H}}/4J)\\
&\quad\times\exp\left(\frac{i\pi}{2}\hat{S}_{2,y}\right)\exp(i\pi\hat{S}_{1,x})\exp\left(\frac{-i\pi}{2}\hat{S}_{2,z}\right)
\end{aligned} \tag{1}$$

The final equality of Eq. (1) can directly be converted into the pulse sequence with two selective $\pi/2$ pulses (with phases x and y) on spin 2, separated by two delays of duration $1/4J$ and a π refocusing in the middle (see Fig. 1). Note that the final selective π pulse on spin 1 just converts the coherence order on spin 1 in Eq. (1) and that the final rotation on Spin 2, a $\pi/2$ z-rotation, does not influence the observed spin 1 coherence. Both pulses can omitted for the pulse sequence design and are not represented in Fig. 1. In contrast to a direct realization of a rotation described by $\hat{S}_1^{\alpha}\hat{S}_{2,y}$ which would require selective manipulation of one line out of the J doublet, the selective pulses in the sequence

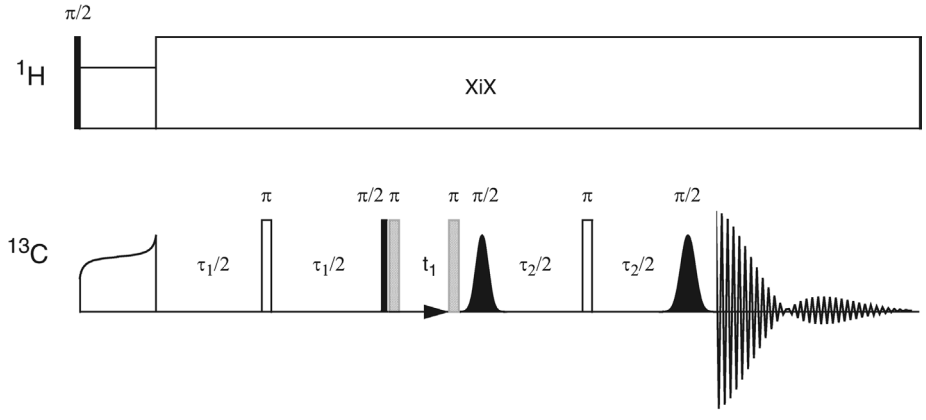

Fig. 1. Pulse sequence for the acquisition of DQ/SQ correlation spectra with DQ generation by INADEQUATE and SSS reconversion of the DQ coherence to observable SQ coherence before t_2 acquisition. Selective reconversion of DQ coherence observable coherence uses $\{x, \bar{x}, y\}$ or $\{x, \bar{x}, \bar{y}\}$ phases for the three pulses in the SSS sequence. Generation of the echo or anti-echo components is obtained by either putting a π pulse directly before or directly after the t_1 evolution delay (hatched pulses).

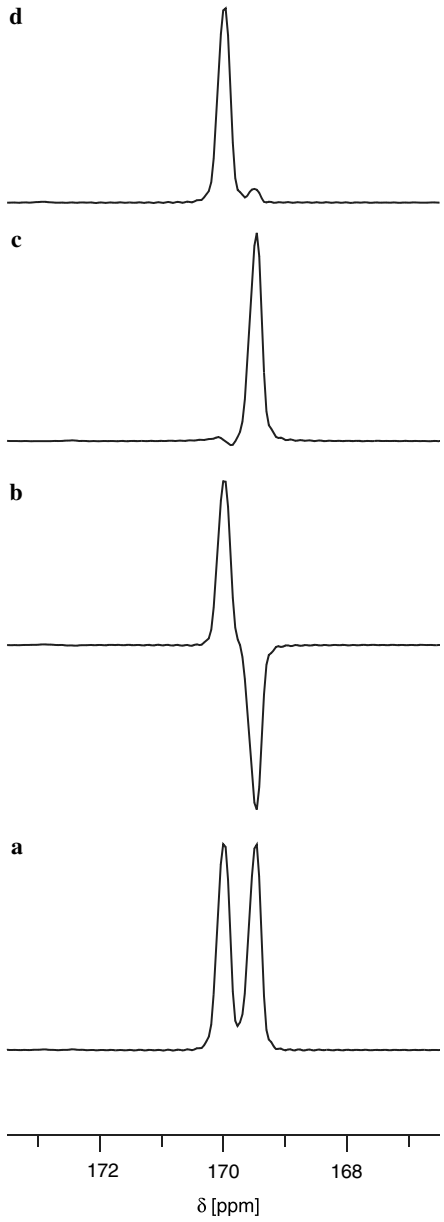

Fig. 2. Carbonyl region of spectra from glycine ethyl ester, ^{13}C labelled at the C′ and C^{α} positions of the glycine moiety of the molecule. (a) CP experiment showing the doublet structure due to the homonuclear J coupling. (b) Standard 1D INADEQUATE with a hard $\pi/2$ reconversion pulse. (c) and (d) 1D INADEQUATE with SSS reconversion to SQ. In (c) the α component of the C′ doublet is selected and in (d) the β component is selected. In both cases the frequency selective $\pi/2$ pulses were centered on the C^{α} region of the spectrum. All spectra (a)–(d) are on the same vertical scale and are the result of the same number of scans. Experiments were performed on a Varian Infinity+ spectrometer operating at a ^{1}H Larmor frequency of 499.734 MHz using a Chemagnetics 2.5 mm TR MAS probe with MAS at 22.50 kHz ± 5 Hz. XiX proton decoupling (pulse width and amplitude: 82.22 μs and 140 kHz). The hard $\pi/2$ and π pulses were 2.5 and 5.0 μs. Frequency selective $\pi/2$ pulse were 270° Gaussian pulses centered on the C^{α} region [39](duration 500 μs, amplitude cut-off at 6.3% of the maximum amplitude). The timing was optimized at $\tau_1 = 8.0$ ms, $\tau_2 = 4.4$ ms. Acquisition: 4096 points with a 12.5 μs dwell. No synchronization between pulse sequence and MAS rotation was attempted. Sixteen scans were taken and no apodisation was applied.

of Fig. 1 are selective to spin 2, and operate on the entire multiplet.

3. Results and discussion

3.1. A model system

The performance of the INADEQUATE-SSS experiment was tested on doubly ^{13}C-labelled glycine ethyl ester. A standard INADEQUATE spectrum shown in Fig. 2b shows an intensity comparable to the CP spectrum of Fig. 2(a) and demonstrates that the DQ generation using J couplings is efficient. The intensity of the selected resonances in the SSS spectra of Fig. 2(c and d) is equal to the corresponding peak in the CP spectrum. This is despite the fact that the SSS part of the experiment adds another 4.4 ms (vide infra) to the INADEQUATE experiment. The explanation for this observation is that the SSS sequence transfers all the DQ coherence to one part of the doublet and in the absence of relaxation the intensity of the selected peak should be twice the intensity of the CP peak.

The SSS spectra also show the efficient selection of a single line of the carbonyl J doublet. Two points are noteworthy: first, the selection of the single component is achieved in a *single* scan. This is a fundamental difference from the IPAP sequence which relies on the addition (or subtraction) of two scans to achieve the selection of a single component [20–23]. The SSS experiment incorporates a DQ filter phase cycle which runs over four scans [31]. However, this cycle is independent of the selection process.

The second point to note is that the optimum delay with respect to the best suppression was found to be significantly shorter than the value predicted from theory. The predicted intensity of the two components of the J doublet with an optimum suppression of the unwanted line at $\tau_2/2 = 1/4J = 3.91$ ms is plotted as a green solid line in Fig. 3(a). The experimental data for the carbonyl resonance of the glycine ethyl ester, also plotted in Fig. 3(a), show a systematic deviation with an optimum suppression already at 2.2 ms. The spectra were recorded under optimized proton-decoupling using XiX [3] with an rf amplitude of 140 kHz. Less efficient decoupling with XiX decoupling at an amplitude of 100 kHz (Fig. 3b) and CW decoupling at 100 kHz (Fig. 3c) accentuates the trend to shorter τ_2 values for optimum suppression. Furthermore, decreased decoupling efficiency leads to a faster decay of the total signal. The diminished initial value is a consequence of faster coherence decay during τ_1. Similar effects on the sensitivity of the spin-state selection process as a function of the quality of the decoupling have been reported in the literature [22]. We note that the optimum value of τ_2 critically depends on the specific parameters of the spin system under consideration, and must be optimized experimentally. The practical applicability in multispin systems will depend on the uniformity of this optimum choice for all spins.

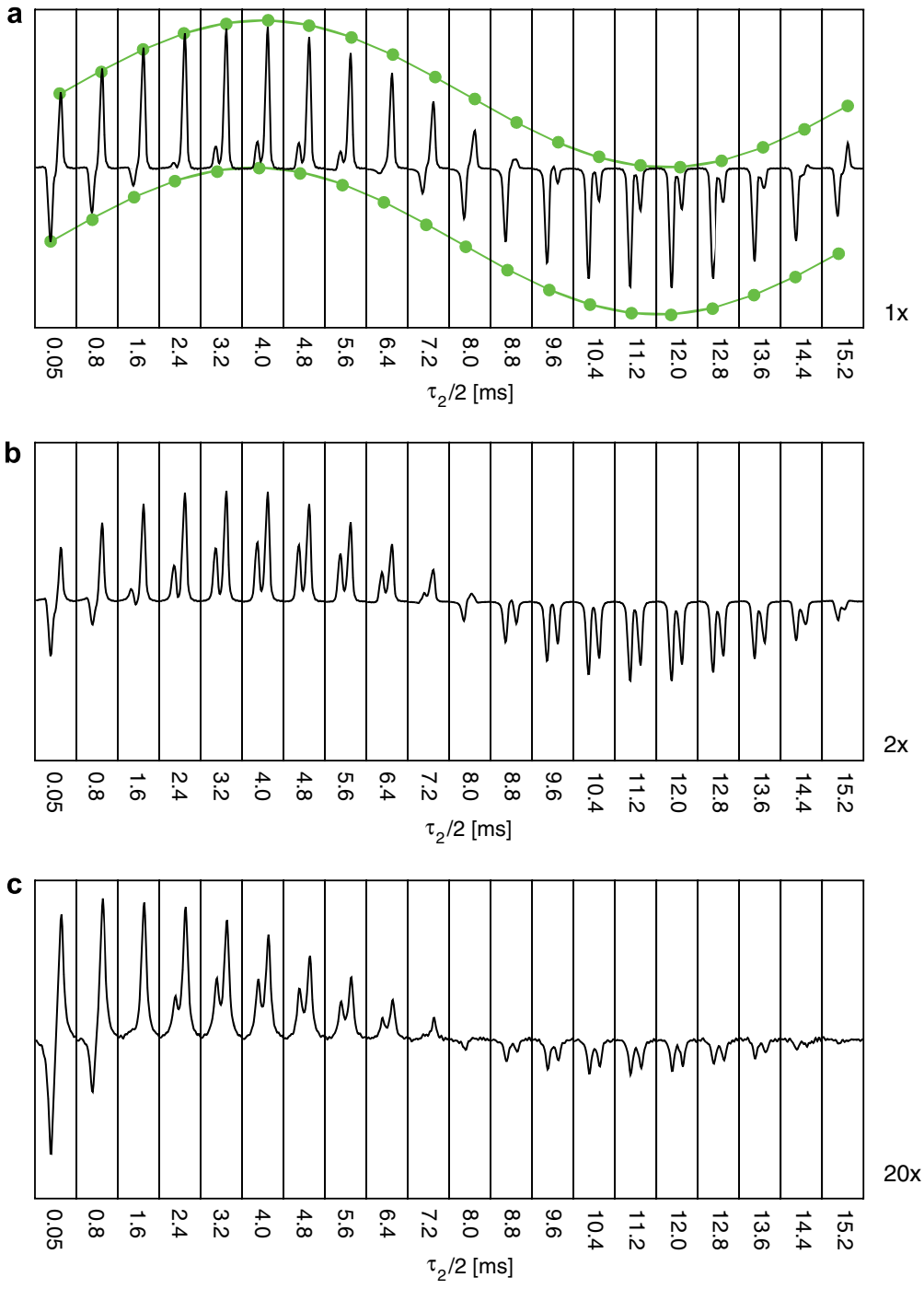

Fig. 3. 1D stack plot of the carbonyl resonance of glycine ethyl ester as a function of the delay τ_2. Results with 140 kHz XiX, 100 kHz XiX, and 100 kHz CW decoupling are shown in (a), (b), and (c), respectively. The vertical scale in (b) is multiplied by a factor of 2 and in (c) by a factor of 20 with respect to the scale in (a). With the exception of the decoupling, all other experimental parameters were the same as those used for the data in Fig. 2. The solid lines (green in online version) in (a) indicate the theoretical expectations for the line intensities in the absence of relaxation processes and using the known *J*-coupling constant. (For interpretation of the references to color in this figure legend, the reader is referred to the web version of this paper.)

3.2. Application to peptides

Figs. 4 and 5 show DQ/SQ spectra of the peptides ubiquitin and HET-s(218–289) obtained with the pulse sequence of Fig. 1. The spectra correlate the isotropic chemical shift of the C′ resonance in the directly detected dimension and the sum of the isotropic shifts of the carbonyl and C^{α} carbons in the indirectly detected dimension. A SQ/SQ correlation representation could be obtained by a shearing transformation [31]. The DQ resonance line is not influenced by the *J* coupling and no homonuclear decoupling is necessary in t_1.

The spectra shown in Figs. 4(b and c) and 5(b and c) are SSS experiments with selection of the α (b panels) and β

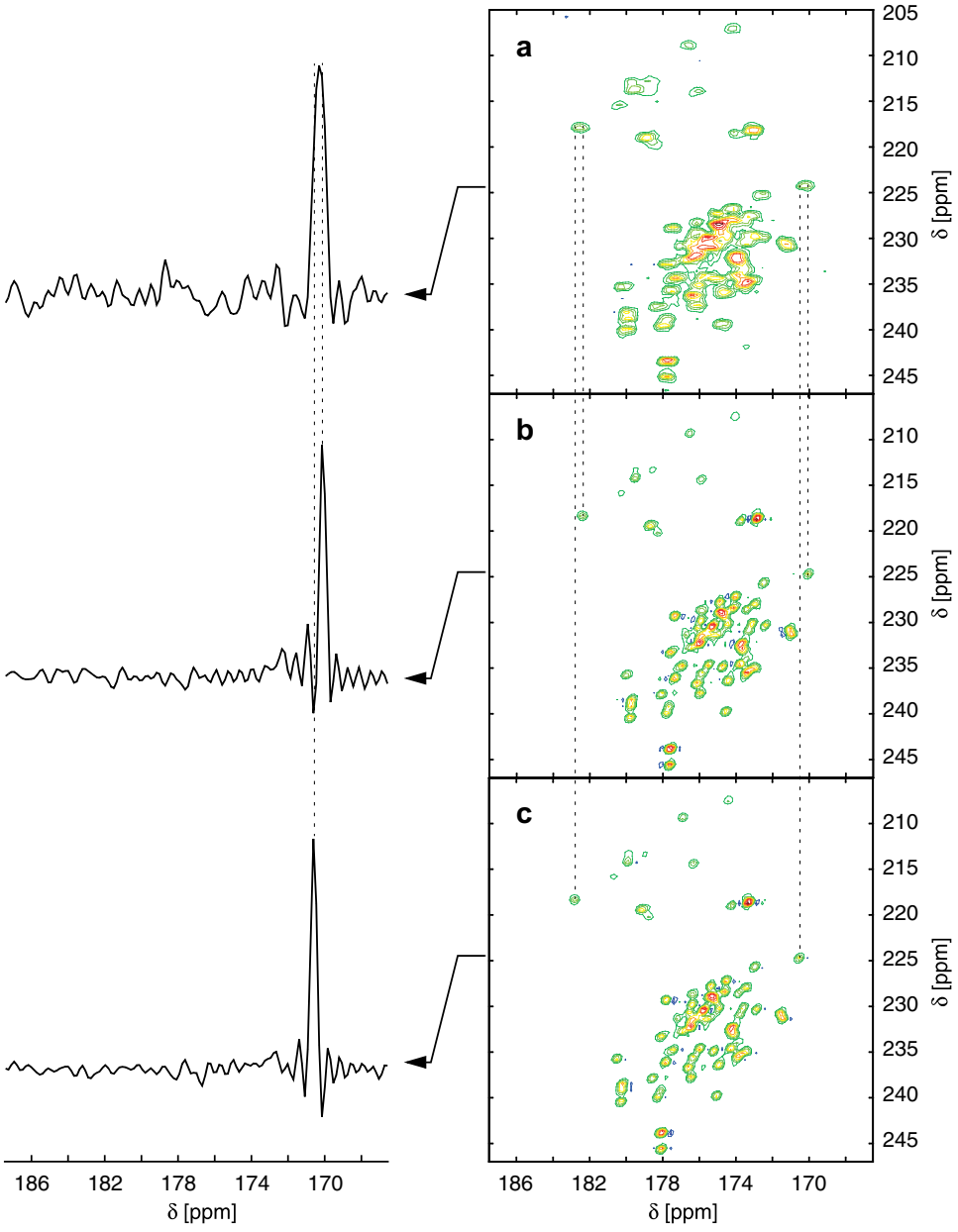

Fig. 4. DQ/SQ correlation spectra of microcrystalline, uniformly ^{15}N, ^{13}C labelled ubiquitin and extracted slices at the indicated positions in ω_2. (a) spectrum acquired with a $R14_4^5$ dipolar excitation and reconversion sequence. (b) and (c) spectra acquired with the SSS sequences shown in Fig. 1 and with a phase of the last pulse to select either the α or β component of the carbonyl doublet respectively. In all figures eight contour levels are draw at 7.5, 14.3, 22.2, 31.6, 42.4, 55.2, 70.1, and 87.5% of the maximum intensity. The MAS rotation frequency was 22.50 ± 0.02 kHz. The non-selective DQ/SQ experiment in (a) was acquired with a $R14_4^5$ DQ recoupling sequence for excitation and reconversion of DQ coherence. Two of these blocks were incorporated in the pulse sequence of Fig. 1 instead of the INADEQUATE and SSS parts. Both excitation and reconversion blocks had a duration of 355.55 ms (28 *R*-elements or 8 rotor cycles). For the experiments in b and c the pulse sequence of Fig. 1 was used. The phase (y or $\bar{y}$) of the final (soft) pulse selected the α or β line. XiX decoupling (Amplitude 106 kHz, pulse length 82.22 μs) was applied. The duration of the Gaussian pulses was 125 μs. The delays $\tau_1/2$ and $\tau_2/2$ were 3.25 and 1.80 ms, respectively. Echo and antiecho spectra with 128 scans per t_1 increment each were averaged with a recycle delay of 3 s. 160 t_1 increments and 512 t_2 points were acquired (dwell 25.0 μs). Total experimental time: 34.4 h. States processing was used. Both the SSS and $R14_4^5$ experiments were zero filled once in the indirect and twice in the direct dimension. A Gaussian line broadening of 16 Hz and 8 Hz was applied in t_1 and t_2. The digital resolution of all spectra after processing is 46.875 Hz/point along ω_1 and 19.53 Hz/point along ω_2. Processing was done in Matlab with the MatNMR toolbox [40]. The spectra were referenced to TMS with an external secondary standard (adamantane).

(c panels) components of the *J* doublet of the carbonyls. The spectra shown in Fig. 4(a) and 5(a) were recorded for comparison and correspond to a DQ/SQ spectrum without spin-state selection. DQ coherence was generated with a dipolar recoupling sequence ($R14_4^5$) for the excitation and reconversion [32,33]. Comparison of the dipolar recoupled data with the data from the SSS experiments, clearly illustrates the increased resolution in the SSS spectra. This is further elaborated by the extracted slices and the vertical dotted lines. In the frequency range between 225 and

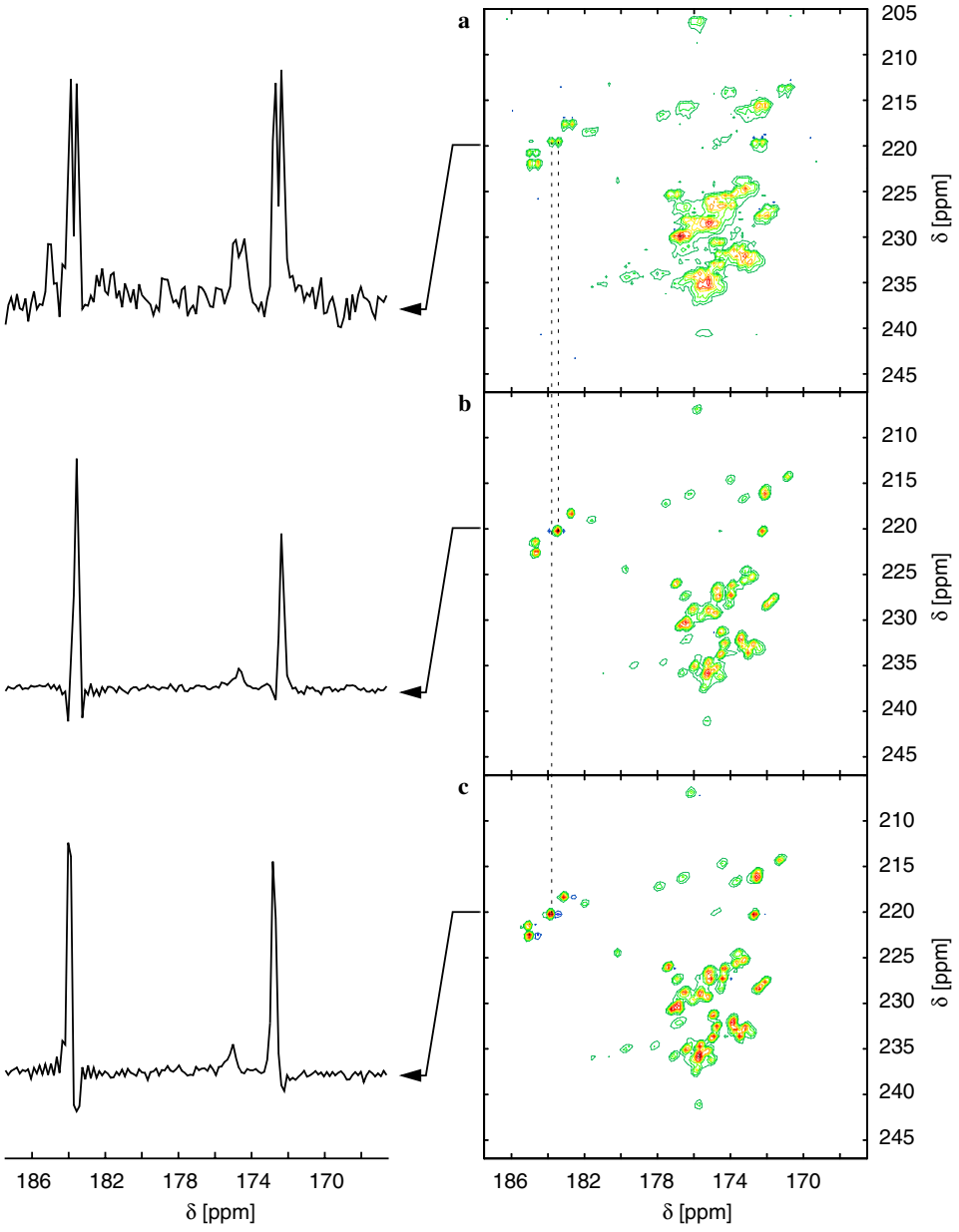

Fig. 5. DQ/SQ correlation spectra of the HET-s (218–289) fragment (U-$^{13}C/^{15}N$) and extracted slices at the indicated position in ω_2. (a) spectrum acquired with a $R14_4^5$ dipolar excitation and reconversion sequence. (b) and (c) spectra acquired with the SSS sequences. Contour levels are set as indicated in Fig. 4. Experimental settings were as indicated in Fig. 4 with the following exceptions: a DR 2.5 mm Bruker probehead was used, XiX amplitude 123 kHz, $\tau_2/2 = 1.90$ ms, 1024 points acquired in t_2.

240 ppm the assignment of resonances to individual correlations is practically impossible in the dipolar spectra, whereas a high percentage of the peaks can actually be identified in the SSS spectra.

In the ubiquitin spectra of Fig. 4(b and c) roughly 50 peaks can be unambiguously picked. Most of these peaks can then actually be assigned to C'–C^{α} correlations of specific residues (not shown) using the published assignments [24,34,35]. Peaks were picked on the basis of a conservative criterion: only those signals which show a maximum in the contour plot were accepted as a peak excluding signals which appear as a shoulder. Strongly overlapping signals were counted as a single signal. The fact that nevertheless 50 peaks can be identified (versus the expected 73 on the basis of the primary structure) illustrates the high resolution of the spectra.

The sensitivity of the experiment when applied to ubiquitin can be evaluated in a similar procedure as for the test compound (Fig. 2). The intensity of the spectrally isolated and well *J*-resolved Met1 carbonyl resonance around 170.5 ppm was used as a benchmark. INADEQUATE, refocused INADEQUATE and INADEQUATE-SSS experiments yielded a signal intensity of 50, 34, and 44%, when compared to a direct CP experiment. The S/N of the ($R14_4^5$) was found to be significantly lower than for SSS experiments (although all data sets were acquired in

roughly the same amount of time). A comparison between J and dipolar transfer is quite involved and outside the scope of this communication.

Fig. 5 shows DQ/SQ spectra of HET-s(218–289). This protein fragment is know to show dynamic heterogeneity with parts of the molecule being highly mobile, and parts being rigid [36,37]. In CP spectra where only the rigid parts are observed, a total of 42 amino acid residues were identified [36]. Using the same procedure as described for ubiquitin, 38 peaks can be picked in the region below 220 ppm in the INADEQUATE-SSS spectra (Fig. 5b and c) and the large majority can immediately be assigned on the basis of the published shifts [38].

4. Conclusions

We have demonstrated that spin-state-selective experiments lead to highly resolved DQ/SQ INADEQUATE correlation spectra for the case of a model system and two polypeptides. The method is shown to work well for spins which have only one coupling partner, such as carbonyl groups in proteins and peptides. Significantly improved resolution in the correlation peaks between C' and C^{α} polypeptide resonances is observed. The single most important experimental parameter is the duration of the reconversion delay as was illustrated experimentally. The optimum length of this delay depends on the experimental settings, and in particular on the quality of the proton decoupling.

Because the usually highly crowded C' and C^{α} region of the protein spectra is of particular importance for the resonance assignment the INADEQUATE-SSS experiments are expected to be of significance for the assignment process in proteins.

Acknowledgments

We acknowledge scientific discussions with Matthias Ernst and Jacco van Beek. We thank Herbert Zimmermann for the synthesis of the selectively labelled glycine ethyl ester. The research was supported by the ETH Zurich through the TH grant system and by the Swiss National Science Foundation (SNF).

References

[1] A.E. Bennett, C.M. Rienstra, M. Auger, K.V. Lakshmi, R.G. Griffin, Heteronuclear decoupling in rotating solids, J. Chem. Phys. 103 (1995) 6951–6958.

[2] B.M. Fung, A.K. Khitrin, K. Ermolaev, An improved broadband decoupling sequence for liquid crystals and solids, J. Magn. Reson. 142 (2000) 97–101.

[3] A. Detken, E.H. Hardy, M. Ernst, B.H. Meier, Simple and efficient decoupling in magic-angle spinning solid-state NMR: the XiX scheme, Chem. Phys. Lett. 356 (2002) 298–304.

[4] G. DePaepe, A. Lesage, L. Emsley, The performance of phase modulated heteronuclear dipolar decoupling schemes in fast magic-angle-spinning nuclear magnetic resonance experiments, J. Chem. Phys. 119 (2003) 4833–4841.

[5] B. Elena, G. de Paepe, L. Emsley, Direct spectral optimisation of proton–proton homonuclear dipolar decoupling in solid-state NMR, Chem. Phys. Lett. 398 (2004) 532–538.

[6] J. Pauli, B. van Rossum, H. Forster, H.J. de Groot, M.H. Oschkinat, Sample optimization and identification of signal patterns of amino acid side chains in 2D RFDR spectra of the alpha-spectrin SH3, J. Magn. Reson. 143 (2000) 411–416.

[7] R.W. Martin, K.W. Zilm, Preparation of protein nanocrystals and their characterization by solid state NMR, J. Magn. Reson. 165 (2003) 162–174.

[8] W. Bermel, I. Bertini, I.C. Felli, M. Piccioli, R. Pierattelli, 13C-detected protonless NMR spectroscopy of proteins in solution, Prog. Nucl. Magn. Reson. Spectrosc. 48 (2006) 25–45.

[9] S.K. Straus, T. Bremi, R.R. Ernst, Resolution enhancement by homonuclear J decoupling in solid-state MAS NMR, Chem. Phys. Lett. 262 (1996) 709–715.

[10] T.I. Igumenova, A.E. McDermott, Improvement of resolution in solid state NMR spectra with J-decoupling: an analysis of lineshape contributions in uniformly ^{13}C-enriched amino acids and proteins, J. Magn. Reson. 164 (2003) 270–285.

[11] H. Matsuo, E. Kupce, H. Li, G. Wagner, Increased sensitivity in HNCA and HN(CO)CA experiments by selective C^{β} decoupling, J. Magn. Reson. Ser. B 113 (1996) 91–96.

[12] H. Matsuo, E. Kupce, G. Wagner, Resolution and sensitivity gain in HCCH-TOCSY experiments by homonuclear C^{β} decoupling, J. Magn. Reson. Ser. B 113 (1996) 190–194.

[13] W. Bermel, I. Bertini, I.C. Felli, R. Kummerle, R. Pierattelli, ^{13}C direct detection experiments on the paramagnetic oxidized monomeric copper, zinc superoxide dismutase, J. Am. Chem. Soc. 125 (2003) 16423–16429.

[14] V. Chevelkov, Z. Chen, W. Bermel, B. Reif, Resolution enhancement in MAS solid-state NMR by application of ^{13}C homonuclear scalar decoupling during acquisition, J. Magn. Reson. 172 (2005) 56–62.

[15] B. Vögeli, H. Kovacs, K. Pervushin, Simultaneous ^{1}H- or ^{2}H-, ^{15}N- and multiple-band-selective ^{13}C-decoupling during acquisition in ^{13}C-detected experiments with proteins and oligonucleotides, J. Biomol. NMR 31 (2005) 1–9.

[16] A. Meissner, T. Schulte-Herbrüggen, J. Briand, O.W. Sørensen, Double spin-state-selective coherence transfer. Application for two-dimensional selection of multiplet components with long transverse relaxation times, Mol. Phys. 95 (1998) 1137–1142.

[17] N.C. Nielsen, H. Thogersen, O.W. Sørensen, A systematic strategy for design of optimum coherent experiments applied to efficient interconversion of double- and single-quantum coherences in nuclear magnetic resonance, J. Chem. Phys. 105 (1996) 3962–3968.

[18] M.D. Sørensen, A. Meissner, O.W. Sørensen, Spin-state-selective coherence transfer via intermediate states of two-spin coherence in IS spin systems: Application to E.COSY-type measurement of J coupling constants, J. Biomol. NMR 10 (1997) 181–186.

[19] R. Verel, J.D. van Beek, B.H. Meier, INADEQUATE-CR experiments in the solid state, J. Magn. Reson. 140 (1999) 300–303.

[20] M. Ottiger, F. Delaglio, J.L. Marquardt, N. Tjandra, A. Bax, Measurement of dipolar couplings for methylene and methyl sites in weakly oriented macromolecules and their use in structure determination, J. Magn. Reson. 134 (1998) 365–369.

[21] P. Andersson, J. Weigelt, G. Otting, Spin-state selection filters for the measurement of heteronuclear one-bond coupling constants, J. Biomol. NMR 12 (1998) 435–441.

[22] L. Duma, S. Hediger, A. Lesage, L. Emsley, Spin-state selection in solid-state NMR, J. Magn. Reson. 164 (2003) 187–195.

[23] L. Duma, S. Hediger, B. Brutscher, A. Bockmann, L. Emsley, Resolution enhancement in multidimensional solid-state NMR spectroscopy of proteins using spin-state selection, J. Am. Chem. Soc. 125 (2003) 11816–11817.

[24] T.I. Igumenova, A.E. McDermott, K.W. Zilm, R.W. Martin, E.K. Paulson, A.J. Wand, Assignments of carbon NMR resonances for microcrystalline ubiquitin, J. Am. Chem. Soc. 126 (2004) 6720–6727.

[25] C. Ritter, M.L. Maddelein, A.B. Siemer, T. Luhrs, M. Ernst, B.H. Meier, S.J. Saupe, R. Riek, Correlation of structural elements and infectivity of the HET-s prion, Nature 435 (2005) 844–848.
[26] O.W. Sørensen, G.W. Eich, M.H. Levitt, G. Bodenhausen, R.R. Ernst, Product operator formalism for the description of NMR pulse experiments, Prog. Nucl. Magn. Reson. Spectrosc. 16 (1984) 163–192.
[27] S. Hediger, B.H. Meier, R.R. Ernst, Adiabatic passage Hartmann–Hahn cross polarization in NMR under magic angle sample spinning, Chem. Phys. Lett. 240 (1995) 449.
[28] A. Lesage, C. Auger, S. Caldarelli, L. Emsley, Determination of through-bond carbon–carbon connectivities in solid-state NMR using the INADEQUATE experiment, J. Am. Chem. Soc. 119 (1997) 7867–7868.
[29] A. Bax, R. Freeman, T.A. Frenkiel, An NMR technique for tracing out the carbon skeleton of an organic-molecule, J. Am. Chem. Soc. 103 (1981) 2102–2104.
[30] A. Bax, R. Freeman, S.P. Kempsell, Natural abundance ^{13}C-^{13}C coupling observed via double-quantum coherence, J. Am. Chem. Soc. 102 (1980) 4849–4851.
[31] R.R. Ernst, G. Bodenhausen, A. Wokaun, Principles of nuclear magnetic resonance in one and two dimensions, Clarendon Press, Oxford, 1987.
[32] A. Brinkmann, M. Eden, M.H. Levitt, Synchronous helical pulse sequences in magic-angle spinning nuclear magnetic resonance: double quantum recoupling of multiple-spin systems, J. Chem. Phys. 112 (2000) 8539–8554.
[33] M.H. Levitt, Symmetry-based pulse sequences in magic-angle spinning solid-state NMR, encyclopedia of NMR, John Wiley & Sons, Ltd, Chichester, 2002.
[34] T.I. Igumenova, A.J. Wand, A.E. McDermott, Assignment of the backbone resonances for microcrystalline ubiquitin, J. Am. Chem. Soc. 126 (2004) 5323–5331.
[35] M. Schubert, T. Manolikas, M. Rogowski, B.H. Meier, Solid-state NMR spectroscopy of 10% ^{13}C labeled ubiquitin: spectral simplification and stereospecific assignment of isopropyl groups, J. Biomol. NMR 35 (2006) 167–173.
[36] A.B. Siemer, C. Ritter, M. Ernst, R. Riek, B.H. Meier, High-resolution solid-state NMR spectroscopy of the prion protein HET-s in its amyloid conformation, Angew. Chem. Int. Ed. 44 (2005) 2441–2444.
[37] A.B. Siemer, A.A. Arnold, C. Ritter, T. Westfeld, M. Ernst, R. Riek, B.H. Meier, Observation of highly flexible residues in amyloid fibrils of the HET-s Prion. J. Am. Chem. Soc. (2006) (early publication on the web).
[38] A.B. Siemer, C. Ritter, M.O. Steinmetz, M. Ernst, R. Riek, B.H. Meier, ^{13}C, ^{15}N resonance assignment of parts of the HET-s prion protein in its amyloid form, J. Biomol. NMR 34 (2006) 75–87.
[39] L. Emsley, G. Bodenhausen, Self-refocusing effect of 270° Gaussian pulses. Applications to selective two-dimensional exchange spectroscopy, J. Magn. Reson. 82 (1989) 211–221.
[40] MatNMR is a toolbox for processing NMR/EPR data under Matlab and can be freely downloaded at http://matnmr.sourceforge.net.